DOI: 10.1002/ejic.200601230

Conformational Analysis of Heteroannularly Substituted Ferrocene Oligoamides

Jasmina Lapić,[a] Daniel Siebler,[b] Katja Heinze,*[b] and Vladimir Rapić*[a]

Keywords: Conformation analysis / Density functional calculations / Hydrogen bonds / Metallocenes / Molecular modelling

The main conformer of symmetrical conjugates of ferrocene-1,1′-dicarboxylic acid with natural amino acids – Fn(CO–$AA_{1–2}$–$OMe)_2$ (type I, Fn = ferrocene-1,1′-diyl, AA = L-α-amino acid) – is supported by two hydrogen bonds between the peptide substituents. To compare intramolecular hydrogen bond patterns of type I conjugates with related asymmetrically substituted derivatives, type II (MeNHCO–Fn–CO–AA–OMe) and type III conjugates (MeNHCO–Fn–CO–AA–NHMe) were prepared in moderate-to-good yields in a few steps starting from 1′-(methoxycarbonyl)ferrocene-1-carboxylic acid by using the HOBt/EDC method (AA = Gly, Ala, Val). ^{1}H NMR spectroscopic variation ratio analysis suggests that an increase in the steric demand of the amino acid side chains favours conformations with hydrogen-bonded FnCO*NH*Me groups. CD spectroscopy of chiral derivatives reveals that (*P*)-helical conformations predominate in solution. The experimental findings are in accordance with DFT calculations.

Introduction

Symmetrically substituted bioconjugates of ferrocene-1,1′-dicarboxylic acid − Fn(CO–AA_n–$OMe)_2$ (Fn = ferrocene-1,1′-diyl, AA = L-α-amino acid, n = 1–2) (type I conjugates) − have been extensively studied, especially with the focus on applications as turn mimetica. Depending on the amino acid employed, these molecules adopt different conformations, A, B or C in the solid state, as well as in solution (Scheme 1).

In the solid state, the majority of type I conjugates form two intramolecular hydrogen bonds, which results in two 10-membered rings (conformation A, β-turn, "Herrick conformation"). If these intramolecular hydrogen bonds are sufficiently strong, conformation A is even retained in chloroform solution.[1–11] The bis(phenylalanine) derivative Fn(CO–Phe–$OMe)_2$ crystallises in asymmetrical form B characterised by a single seven-membered intramolecular hydrogen-bonded ring (γ-turn, "van Staveren conformation"), whereas conformation A presumably predominates in solution.[12] The derivatives Fn(CO–AA–$OMe)_2$ (AA = Pro, Cys(Bzl), Val) provide examples of open "Xu conformations" C in the solid state.[13–16] However, conformations found in the solid state can be substantially different from solution conformations as intermolecular hydrogen bonds are usually additionally present in the solid state. Therefore, with respect to chemical reactivity, the conformations adopted in solution are of importance. A systematic description of the structural motifs and a suitable nomenclature of 1,1′-disubstituted ferrocenes has been recently put forward.[17]

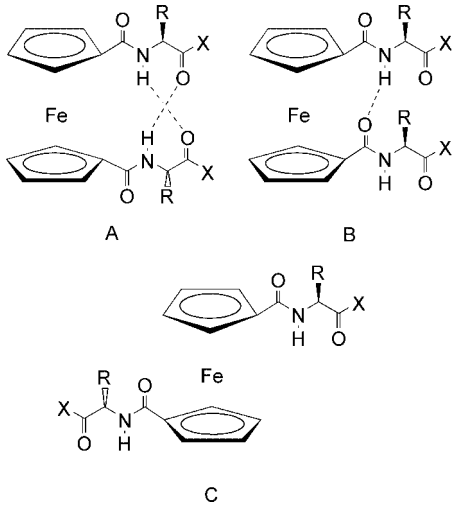

Scheme 1. Intramolecular hydrogen bond patterns in symmetrical ferrocene peptides (type I) [X = OMe, L–AA–OMe].

Having in mind the conformational characteristics of type I conjugates, we aimed to investigate the hydrogen bonding patterns of related asymmetrically substituted derivatives of ferrocene-1,1′-dicarboxylic acid belonging to

[a] Department of Chemistry and Biochemistry, Faculty of Food Technology and Biotechnology,
Pierottijeva 6, 10000 Zagreb, Croatia
Fax: +385-4836-082
E-mail: vrapic@pbf.hr
[b] Department of Inorganic Chemistry, University of Heidelberg,
Im Neuenheimer Feld 270, 69120 Heidelberg, Germany
Fax: +49-6221-545707
E-mail: katja.heinze@urz.uni-heidelberg.de
Supporting information for this article is available on the WWW under http://www.eurjic.org or from the author.

type II (MeNHCO–Fn–CO–AA–OMe) and type III (MeNHCO–Fn–CO–AA–NHMe) (AA = Gly, L-Ala, L-Val) to understand individual conformational preferences in solution with respect to the amino acid employed (i.e. the size of their side chains). Here we describe the conformational analyses based on a combined experimental (NMR, IR and CD spectroscopy) and theoretical approach (DFT calculations).

Results and Discussion

Scheme 2 depicts three possible hydrogen bonded conformations, D, E and F, with (*P*)-helical stereochemistry at the ferrocene as well as an open form of type II conjugates. The corresponding (*M*)-helical diastereomeric conformations can be derived from the mirror images and by changing the resulting D-configuration of the amino acid to L. Descriptor "1-" denotes the amino acid containing the substituent and descriptor "1′-" denotes the CONHMe part of the compounds. Conformations D and E can be described by seven-membered "van Staveren"-like intramolecular hydrogen bonds (Scheme 1, B), whereas form F is stabilised by a 10-membered intramolecular hydrogen bonded ring, which can be considered as half of a "Herrick's" motive (Scheme 1, A). These patterns represent γ- and β-turn structures, and it is expected that their relative population depends on the

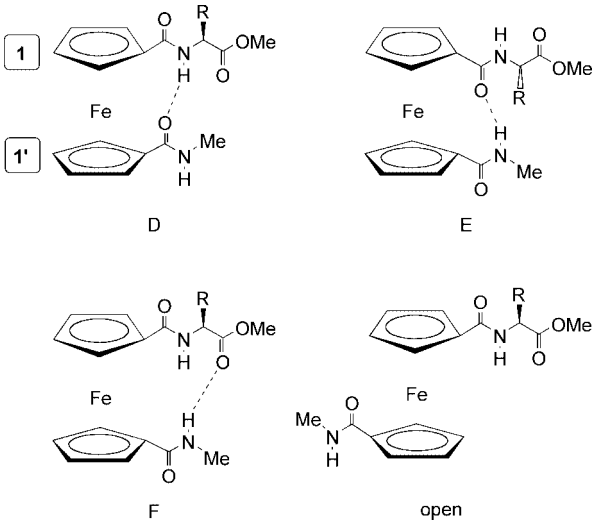

Scheme 2. Possible intramolecular hydrogen bond patterns in diamide esters (type II).

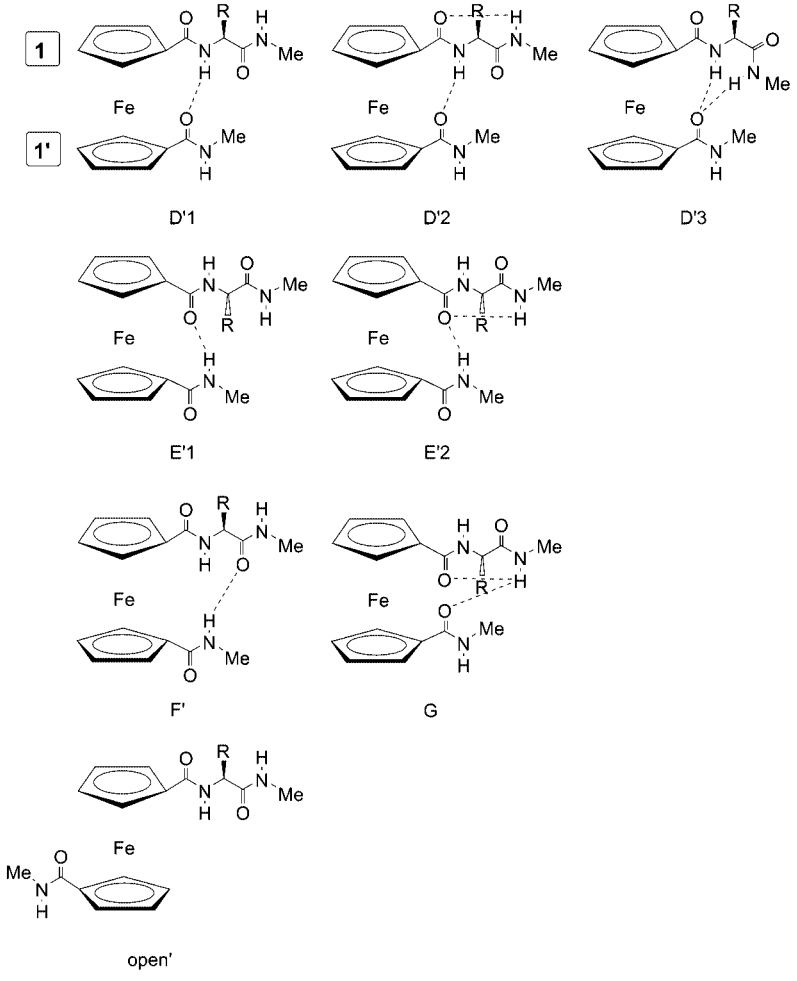

Scheme 3. Possible intramolecular hydrogen bond patterns in triamides (type III).

steric demand of the amino acid side chain (R). Conformation E was recently observed in the solid state and in a $CDCl_3$ solution of 1′-(butylcarbamoyl)-*N*-morpholinoferrocene-1-carboxamide.[18]

Intramolecular hydrogen bonding patterns possible in type III conjugates are shown in Scheme 3. Three conformations are analogous to forms D, E and F of amide esters and for clarity, they are denoted as D′, E′ and F′. However, owing to the additional 1-NHMe group, a further hydrogen bond between 1-NHMe and 1-CO in D′2, E′2 and F′ or between 1-NHMe and 1′-CO in D′3 is possible. In theoretically possible conformation G, a 10-membered hydrogen bonded ring between 1′-CO and 1-NHMe occurs together with an intrachain hydrogen bond between 1-NHMe and 1-CO. Thus, the conformational space of type III conjugates is considerably expanded relative to type II conjugates.

Synthesis of Type II and Type III Conjugates

The syntheses of diamide esters **9**–**11** and triamides **15**–**17** are depicted in Scheme 4. The starting compound, 1′-(methoxycarbonyl)ferocene-1-carboxylic acid (**6**), was prepared according to a previously described procedure.[30] Activation of acid **6** with HOBt/EDC (HOBt = 1-hydroxybenzotriazole, EDC = *N*-(3-dimethylaminopropyl)-*N*′-ethylcarbodiimide hydrochloride) in CH_2Cl_2 solution, followed by treatment with NH_2Me (obtained from $NH_2Me{\cdot}HCl$ and NEt_3) gave 45% of methyl 1′-(methylcarbamoyl)ferrocene-1-carboxylate (**7**). Amide ester **7** was hydrolysed with $NaOH/H_2O$ in MeOH to give 1′-(methylcarbamoyl)ferrocene-1-carboxylic acid (**8**) (97% yield). Acid **8** was activated by HOBt/EDC and coupled with Gly–OMe, L-Ala–OMe, D-Ala–OMe and L-Val–OMe (obtained from AA–OMe·HCl by treatment with NEt_3), which resulted in the formation of diamide esters **9** (42%), **10** (60%), **10a** (54%) and **11** (46%), respectively. Hydrolysis of diamide esters **9**–**11** gave MeNHCO–Fn–CO–AA–OH in good yields [**12** (94%), **13** (81%) and **14** (94%)] which were subsequently transformed into triamides **15** (24%) **16** (56%) and **17** (20%), respectively, in a manner analogous to that described for the preparation of **7**. Unexpectedly, compounds **16** and **17** thus obtained had racemized during hydrolysis as they displayed only a negligible Cotton effect (in contrast to **10** and **11**, Table 6). Therefore, **8** was directly coupled with AA–NHMe (AA = Gly, L-Ala, L-Val) to give triamide **15** (45%), as well as optically pure triamides **16** (45%) and **17** (34%).

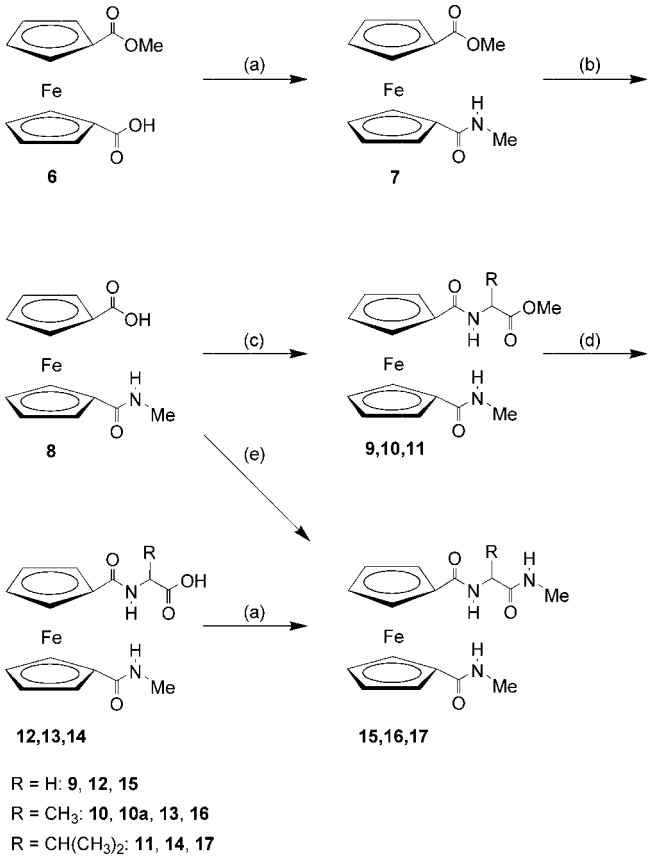

Scheme 4. Synthesis of $Fn(COOH)_2$-derived oligoamides. a) 1. HOBt/EDC, CH_2Cl_2, 2. $NH_2Me{\cdot}HCl$, NEt_3, CH_2Cl_2; b) $NaOH/H_2O$, MeOH; c) 1. HOBt/EDC, CH_2Cl_2, 2. L-AA–OMe·HCl, NEt_3, CH_2Cl_2; d) $NaOH/H_2O$, dioxane; e) 1. HOBt/EDC, CH_2Cl_2, 2. L-AA–NHMe·HCl, NEt_3, CH_2Cl_2.

Spectroscopy of Type II and Type III Conjugates

Intramolecular hydrogen bonds found in the solid state often undergo cleavage even in weakly coordinating solvents (e.g. chloroform, dichloromethane) with competitive formation of hydrogen-bond-free states and species with hydrogen bonded rings of different sizes. The conformational equilibria are usually fast on the NMR timescale, which results in time-averaged and population-weighted chemical shifts, but in some cases, barriers are high enough to allow the detection of individual conformers or conformer groups.[19] On the faster IR timescale, however, absorptions for NH and CO stretching vibrations are detected for each conformer present in solution (unfortunately with severe overlap, which often precludes detailed assignment).[20] In chiroptical experiments (CD spectroscopy) the measured signal represents the sum of signals for all species present in solution.

To elucidate the conformational equilibria of **9**–**11** and **15**–**17** in solution and to probe the influence of the amino acid side chain [R = H, CH_3, $CH(CH_3)_2$], we used IR and CD spectroscopy, NMR spectroscopy (solvent-dependent, temperature-dependent) and DFT calculations (B3LYP, LanL2DZ[19,21–24]).

IR spectra of **7**, **9**–**11** and **15**–**17** were measured in CH_2Cl_2 solution at different concentrations (Table 1). The characteristic signals (NH, CO) were unchanged in the concentration range 0.5×10^{-2} to 2.5×10^{-2} M, which confirms

that intermolecular interactions are absent under these conditions. Signals for non-hydrogen-bonded NH groups as well as hydrogen bonded NH groups are observed. For **7**, the low-energy CO_{ester} absorption indicates a quite strong hydrogen bond from 1′-NH to the ester carbonyl group, which corresponds to the only possible hydrogen bonded conformation E. Thus, **7** exists in solution as conformer E in equilibrium with the open form.

Table 1. IR data [cm^{-1}] for **7**, **9**–**11** and **15**–**17** in CH_2Cl_2 (c = 10^{-2} M).

	ν_{NH} (free)	ν_{NH} (assoc.)	ν_{CO} (ester)	ν_{CO} (amide I)
7	3462	3373	1712	1659
9	3446, 3391	3259	1742	1650
10	3451	3271	1740	1650
11	3453, 3418	3293	1736	1665
15	3449	3341	–	1655
16	3449	3363, 3327	–	1653
17	3451	3342, 3326	–	1657

Chiral amide esters **10** and **11** display Cotton effects at about 350 (300 nm), –275 (348 nm), –155 (411 nm), and 395° $M^{-1}cm^{-1}$ (470 nm) in acetonitrile. For chiral triamides **16** and **17**, the following Cotton effects were observed: 825 (305 nm), –410 (352 nm), –230 (417 nm) and 470° $M^{-1}cm^{-1}$ (480 nm) (Experimental Section, Table 6). The spectra are very similar to those of type I derivatives with "Herrick conformations" (Scheme 1, A). A positive Cotton effect around the ferrocene absorption ($\lambda_{max} \approx 440$ nm; Experimental Section, Table 6) was previously interpreted as being indicative of (*P*)-enantiomers of the helically ordered ferrocenes.[9,17] However, the CD intensities of **10**, **11**, **16** and **17** are one order of magnitude lower than those found for type I (*P*)-helical "Herrick conformations" (Scheme 1, A; $M_\theta \approx$ 5000° $M^{-1}cm^{-1}$) with two intramolecular hydrogen bonds between the L-amino acid side arms. Thus, CD spectroscopy of L-amino acid derivatives suggests that (*P*)-helical conformations are present in slight excess over (*M*)-helical and open conformations, whereas (*M*)-helical conformations are slightly preferred for D-Ala derivative **10a** (Figure 1, Experimental Section, Table 6). As expected, CD spectra of amide esters **10** and **10a** derived from L- and D-Ala, respectively, are mirror images of each other (Figure 1). Interestingly, the positive Cotton effects increase for amide esters **10** and **11** from 360 to 430° $M^{-1}cm^{-1}$ (470 nm) as well as for triamides **16** and **17** from 410 to 530° $M^{-1}cm^{-1}$ (480 nm). This slight enhancement could be attributed to an increased amount of (*P*)-helical ferrocenes present in solution, which results from an increase in the size of the amino acid side chain from R = CH_3 to R = $CH(CH_3)_2$.

To address the engagement of specific NH protons (1-NH, 1′-NH, 1-NHMe) in hydrogen bonding by ^1H NMR spectroscopy, all the NH proton signals have to be correctly assigned. NOE spectroscopy allowed all NH proton signals to be distinguished as specific NOE cross peaks are observed to cyclopentadienyl protons and CH_α of the amino acid as shown exemplarily for **16** in Figure 2. NH protons

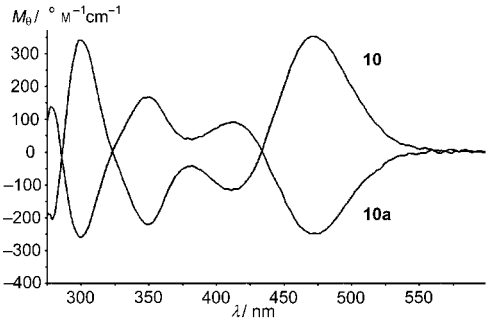

Figure 1. CD spectra of **10** and **10a** in CH_3CN.

adjacent to ferrocene carbonyl (1-NH, 1′-NH) display NOE cross peaks to two Cp protons, while 1-NHMe shows an NOE contact to CH_α.

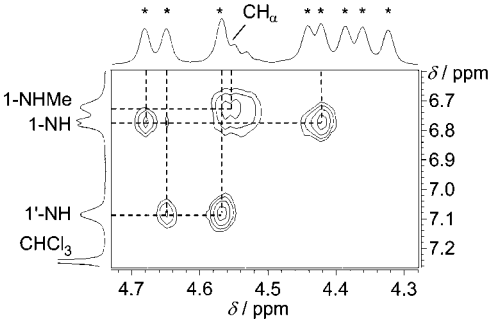

Figure 2. Part of the NOESY spectrum of **16**, which indicates NOE contacts between NH protons and Cp-H and CH_α (* denotes Cp-H).

To address the question as to which NH group preferentially participates in hydrogen bonds, NH chemical shifts were measured in different solvents ["variation ratio" (v.r.) method][25] and at different temperatures (VT ^1H NMR spectroscopy). For interpretation of the observed δ_{NH} values, it has proven useful to compare them to those of standard (reference) compounds. The standard compounds possess NH groups in a comparable chemical environment but without any intramolecular hydrogen bonds (non-hydrogen-bonded reference state) in noncoordinating solvents (e.g. $CDCl_3$). The fully hydrogen-bonded reference state is simulated by measuring the ^1H NMR spectrum in the strongly coordinating solvent [D_6]DMSO (Experimental Section, Tables 4 and 5).

Chemical shift variation from [D_6]DMSO to $CDCl_3$ ($\Delta\delta_{NH}$) provides a measure of the extent to which an amide proton takes part in an intramolecular hydrogen bond. If the shift variation of a particular NH proton is distinctly smaller than that of the hydrogen-bond-free reference, the NH proton is considered to be intramolecularly hydrogen bonded in $CDCl_3$ solution. The variation ratio v.r. = $\Delta\delta_{NH}$(substrate)/$\Delta\delta_{NH}$(reference) describes the involvement of the considered proton in an intramolecular hydrogen bond. Small v.r. values indicate strong hydrogen bonds whereas larger v.r. values suggest weak hydrogen bonds.[25] We, and others, have previously synthesised a number of peptides derived from 1′-aminoferrocene-1-carboxylic acid

Table 2. ^{1}H NMR spectroscopic data for **7**, **9**–**11**, **15**–**17** and standard (reference) compounds ($c = 5\times10^{-3}$ to 2×10^{-4} M).[a]

	δ_{NH} / ppm ($CDCl_3$)[b]			δ_{NH} / ppm ([D_6]DMSO)[b]			$\Delta\delta$ / ppm ([D_6]DMSO/$CDCl_3$)			v.r. (standard)			$-\Delta\delta/T$[c] / ppb K^{-1}		
1	5.43			7.71			2.37								
2	6.08			8.25			2.17								
3	6.02			8.23			2.21								
4	5.90			8.08			2.18								
5	5.73			7.73			2.00								
7	6.10			7.75			1.65			0.83 (**5**)					
9	6.72	7.39		7.73	8.40		1.01	1.01		0.51 (**5**)	0.47 (**2**)		7.0	16.0	
10	6.88	7.03		7.75	8.24		0.87	1.21		0.44 (**5**)	0.55 (**3**)		7.0	8.4	
11	7.03	6.63		7.66	7.88		0.63	1.25		0.32 (**5**)	0.57 (**4**)		[d]		
15	6.89	7.15	6.86	7.98	8.17	7.85	1.09	1.02	0.99	0.55 (**5**)	0.47 (**2**)	0.42 (**1**)	6.1	0.4	8.9
16	7.08	6.77	6.71	7.97	7.88	7.91	0.89	1.11	1.20	0.45 (**5**)	0.50 (**3**)	0.51 (**1**)	18.9	7.9	11.5
17	7.20	6.52	6.55	7.88	7.65	8.01	0.68	1.13	1.46	0.34 (**5**)	0.52 (**4**)	0.62 (**1**)	11.8	2.6	10.9

[a] All values are given in the sequence 1′-NH, 1-NH and 1-NHMe. [b] δ_{NH} ($CDCl_3$) and δ_{NH} ([D_6]DMSO) for compounds **1**–**5** are taken from refs.[25,26] [c] 1.0×10^{-4} M in $CDCl_3$. [d] Sample precipitates under these conditions.

(Fca)[21,27] and natural amino acids.[19,24,26,28,29] In this context, we have successfully employed the v.r. method in the estimation of intramolecular hydrogen bond strengths and conformer populations in Fca–AA conjugates.[24,26]

Suitable reference compounds for amide esters **9**–**11** are Ac–AA–OEt (AA = Gly, Ala, Val; **2**–**4**) for the amino acid containing substituent in position 1- and *N*-methylferrocenecarboxamide Fc–CONHMe (**5**) for the 1′-NHMe part. For the 1-NHMe moiety of triamides **15**–**17**, *N*-methylacetamide (MeCONHMe, **1**) is used as a reference compound. As mentioned above, the reference compounds are unable to engage in intramolecular hydrogen bonds and exhibit chemical shifts of the amide protons at positions well below $\delta = 7$ ppm in $CDCl_3$. In [D_6]DMSO solution, the signals are shifted to lower field ($\delta \approx 8$ ppm), which indicates intermolecular hydrogen bonds to the solvent ($\Delta\delta_{NH} \geq 2.0$ ppm, Table 2).

To exemplify this approach, v.r. calculations for ester amide **9** will be described. In $CDCl_3$ solution, compound **9** exhibits amide resonances at $\delta = 6.72$ ppm for 1′-NH and $\delta = 7.39$ ppm for 1-NH groups (unambiguously assigned by NOESY experiments and coupling patterns). In [D_6]-DMSO, the corresponding resonances appear at $\delta = 7.73$ ppm and $\delta = 8.40$ ppm (Figure 3). The difference in the chemical shifts of the two amide protons in the two solvents is $\Delta\delta = 1.01$ ppm for both protons. A suitable standard (reference) for 1′-NH is FcCONHMe (**5**) with $\Delta\delta = 2.00$ ppm, and for 1-NH Ac–Gly–OEt (**2**) with $\Delta\delta = 2.17$ ppm was chosen. Thus, v.r. (1′-NH) = 0.51 and v.r. (1-NH) = 0.47 can be calculated for **9**, and these values indicate medium–strong hydrogen bonds for both protons. This finding can only be explained by the presence of several conformations which are in equilibrium in solution. As only conformer D possesses a hydrogen bonded 1-NH group, this species is surely present in solution, whereas the v.r. data do not discriminate between conformations E and F as both possess 1′-NH involved in hydrogen bonds (Scheme 2).

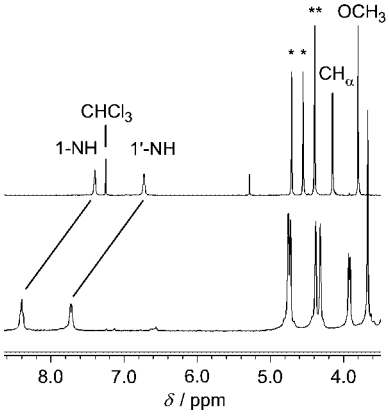

Figure 3. Part of the ^{1}H NMR spectra of **9** in $CDCl_3$ (top) and [D_6]DMSO (bottom) (* denotes Cp-H).

In the sequence **9**, **10**, **11**, a monotonous lowering of v.r. values of the 1′-NH protons occurred ($0.51 > 0.44 > 0.32$), which indicates an enrichment of conformations E and/or F displaying 1′-NH···O bonds. Concomitantly, conformations with 1-NH···O bonds (D) are less populated (v.r. values: $0.47 < 0.55 < 0.57$). Similar to amide esters **9**–**11**, in the order **15**, **16**, **17**, v.r. values for 1′-NH protons decrease ($0.55 > 0.45 > 0.34$) and increase for 1-NH protons ($0.47 < 0.50 < 0.52$). 1-NHMe protons show increasing v.r. values ($0.34 < 0.52 < 0.62$). Once again, these findings indicate enrichment of E′ and/or F′ forms at the expense of conformers D′ and G (Scheme 3).

Additionally, variable temperature NMR experiments were undertaken in $CDCl_3$ solution (Figure 4). However, valine derivative **11** visibly precipitates upon cooling (presumably by association through intermolecular hydrogen bonds). For **9** and **16**, the large temperature shifts $\Delta\delta/T$ of NH protons are indicative of beginning intermolecular hydrogen bonding upon cooling (Table 2). Thus, temperature shifts $\Delta\delta/T$ of **9**, **16** and **17** are clearly not interpretable in

terms of intramolecular hydrogen bonding. Thus, for **10** and **15**, it should also be considered that intermolecular interactions (especially through 1′-NH and 1-NHMe) are highly probable at lower temperatures.

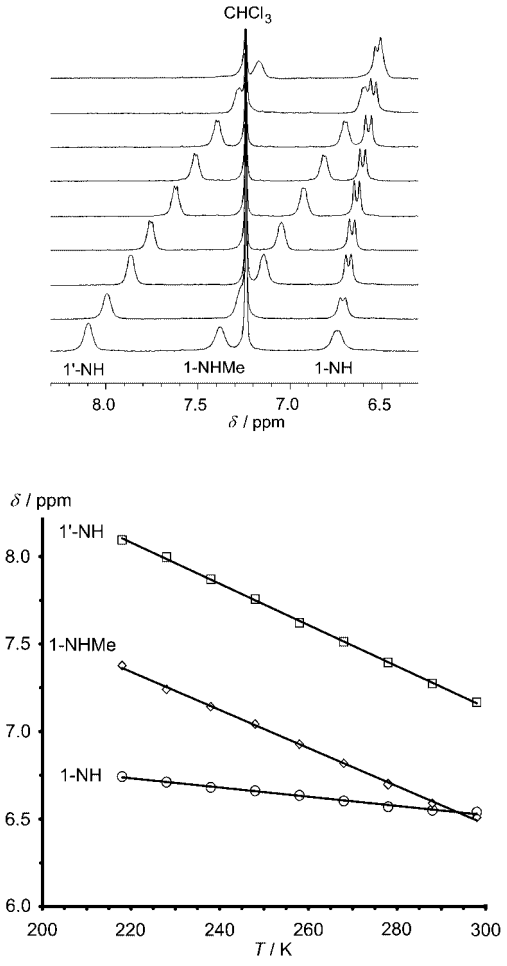

Figure 4. Partial VT ^{1}H NMR spectra of **17** in $CDCl_3$ (top) and δ versus T plot of the amide protons.

The combined experimental data can be summarised as follows: (1) chiral L-amino acid conjugates form predominantly (*P*)-helical conformations in solution for both type II and III conjugates, (2) all NH protons are involved in intramolecular hydrogen bonding in the ensemble, (3) according to NH v.r. values for types II and III, increasing the steric bulk of the amino acid side chain (R) results in a larger fraction of conformers with 1′-NH···O hydrogen bonds and a smaller fraction of conformers with 1-NH···O hydrogen bonds, (4) for type III conjugates, an increase in the steric bulk of the amino acid side chain (R) leads to a depletion of conformers with 1-NHMe···O hydrogen bonds in the ensemble.

DFT Calculations

To gain deeper insight into the possible conformations, the geometries of compounds **9**–**11** and **15**–**17** were optimised by DFT calculations without symmetry constraints (B3LYP, LanL2DZ) in different conformations, that is, with respect to hydrogen bonding patterns (D, E, F, open, D′, E′, F′, G′ and open′) and ferrocene helicity (*P*, *M*) (Table 3, Figures 5 and 6). In all cases, the open form is calculated to be higher in energy by 13–19 kJ mol^{-1} relative to the calculated minimum geometry. Type II compounds **9**–**11** with two hydrogen-donors and three hydrogen-acceptors will be discussed before type III conjugates **15**–**17** with three donors and three acceptors are addressed.

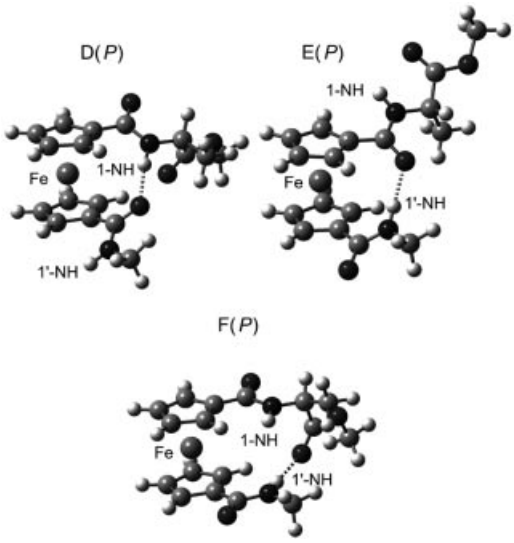

Figure 5. DFT-calculated (*P*)-helical minimum structures of **10**.

For glycine derivative **9**, all conformations D, E and F are local minima with marginal energy differences, which confirms that no conformation is especially preferred over the others and also substantiates conclusion (2) above. In sterically more demanding conjugates **10** and **11**, conformations D(*M*) and F(*M*) are destabilised by the larger substituent R (Figure 7). Thus, less (*M*)-helical ferrocenes equalling more (*P*)-helical conformers are present in the ensemble in accordance with conclusion (1) above. According to the calculations, the ensemble is enriched in E conformers as D(*M*) and F(*M*) are energetically unfavourable for **10** and **11**. Conformers E exhibit 1′-NH···O hydrogen bonds, which accounts for conclusion (3). Additionally, F(*P*) becomes the most stable conformation for **11**, which also shows 1′-NH···O hydrogen bonds and furthermore explains the lower $C{=}O_{ester}$ stretching vibration frequency of **11** relative to that of **9** (Table 1).

Type III conjugates show a more complicated behaviour as the number of possible conformations with hydrogen bonds has doubled relative to type II compounds. No stable minimum structure could be obtained for the G conformation shown in Scheme 3 as the 1-NHMe···1′-CO hydrogen bond is disrupted, which leaves only the intrachain hydrogen bond between 1-NHMe and 1-CO. This conformation is almost as high in energy as the open form and rules out a significant contribution (Table 3). Glycine conjugate **15** shows no conformational preference as does its type II counterpart **9**, that is, all conformations D′1, D′2, D′3, E′1, E′2 and F′ with (*P*) and (*M*) helical ferrocenes are present

Table 3. DFT calculated relative energies and (N)H···O distances of hydrogen bonds of conformers for **9**–**11** and **15**–**17**.

	E_{rel} / kJ mol^{-1}	(N)H···O / Å (interchain)	(N)H···O / Å (intrachain)
9D	0.6	1.87	–
9E	0.0	1.93	–
9F	3.9	2.00	–
9-open	13.4	–	–
10D(*P;M*)	0.0; 12.0	1.89; 1.87	–; –
10E(*P;M*)	0.4; 0.7	1.93; 1.93	–; –
10F(*P;M*)	3.7; 17.2	1.99; 1.97	–; –
10-open	13.6	–	–
11D(*P;M*)	7.8; 25.6	1.96; 1.87	–
11E(*P;M*)	1.7; 2.4	1.93; 1.93	–; –
11F(*P;M*)	0.0; 25.5	2.00; 2.16	–; –
11-open	15.0	–	–
15D′1	7.3	1.86	–
15D′2	0.0	1.85	1.93
15D′3	9.1	2.17, 1.90	–
15E′1	1.9	1.91	–
15E′2	5.5	1.97	2.03
15F′	7.0	1.99	(2.45)
15G	16.2	–	1.97
15open′	17.1	–	–
16D′1(*P;M*)	–; –	–; –	–; – (both converged to 16D′2)
16D′2(*P;M*)	0.0; 8.7	1.87; 1.85	1.94; 1.84
16D′3(*P;M*)	10.6; 13.1	2.16, 1.92; 1.96, 1.94	–
16E′1(*P;M*)	6.6; 6.4	1.92; 1.92	–
16E′2(*P;M*)	1.7; 18.5	1.94; 1.96	2.03; 1.90
16F′(*P;M*)	5.9; 18.9	1.98; 1.93	(2.60); (3.06)
16G(*P;M*)	14.4; 30.9	–; –	2.01; 1.92
16open′	16.7	–	–
17D′1(*P;M*)	13.5; –	1.99; –	–; – (the latter converged to 17D′2(M)
17D′2(*P;M*)	0.0; 5.0	1.86; 1.85	2.00; 1.84
17D′3(*P;M*)	12.7; 15.7	2.13, 1.92; 1.97, 1.93	–
17E′1(*P;M*)	7.6; 6.3	1.93; 1.92	–; –
17E′2(*P;M*)	3.4; 12.4	1.95; 1.96	2.10; 1.91
17F′(*P;M*)	2.9; 14.7	1.97; 2.05	(2.48); 2.06
17G(*P;M*)	17.0; 44.6	–; –	1.89; 1.89
17open′	19.4	–	–

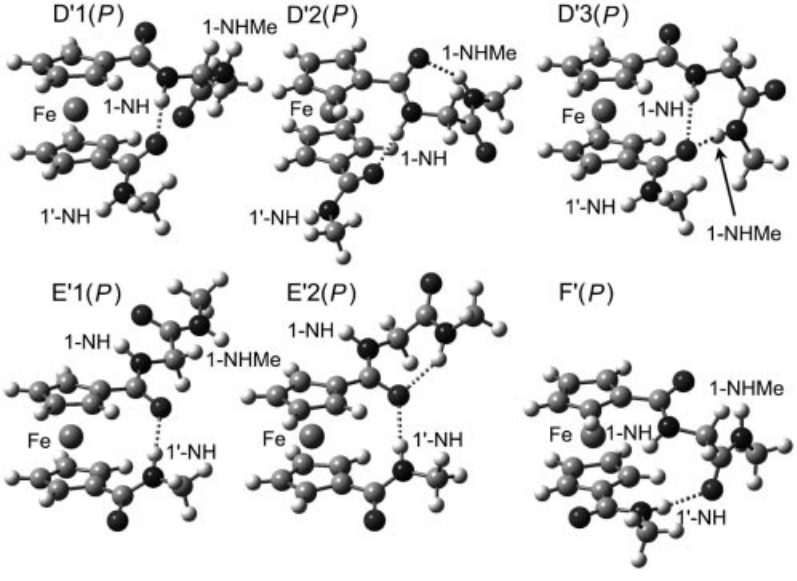

Figure 6. DFT-calculated (*P*)-helical minimum structures of **15**.

in the ensemble (Figure 7). An increase in the size of R in the L-amino acid destabilises conformations D′1(*P*), D′1(*M*), D′3(*P*), D′3(*M*), E′2(*M*) and F′(*M*). Thus, in the ensemble, conformers D′2(*P*), D′2(*M*), E′1(*P*), E′1(*M*), E′2(*P*) and F′(*P*) are still present, which results in an excess of (*P*)-helical ferrocenes for **16** and **17** and corroborates

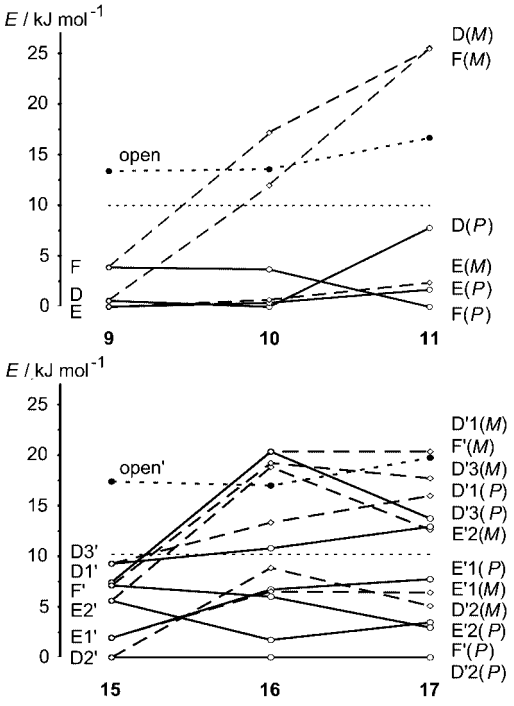

Figure 7. Relative energies of conformations of type II conjugates **9**–**11** (top) and of conformations of type III conjugates **15**–**17** (bottom) [for 16D′1(*P*), 16D′1(*M*) and 17D′1(*M*), the relative energy must be arbitrarily set to 20 kJ mol^{-1}; the dotted lines at 10 kJ mol^{-1} are a guide for the eye].

conclusion (1) above. Analogously to type II conjugates, the ensembles of **16** and **17** contain more E conformers relative to the ensemble of glycine derivative **15**. This confirms conclusion (3), which states that a larger fraction of conformers with 1′-NH···O hydrogen bonds exists for derivatives with larger R substituents. As for type II derivatives, F′(*P*) conformations (with 1′-NH···O hydrogen bonds) are increasingly stabilised by larger R side chains.

Interchain 1-NHMe hydrogen bonds are only present in conformations D′3 and G (Scheme 3), which are quite high in energy. Thus, 1-NHMe hydrogen bonds are mainly intrachain in nature and occur in conformations D′2, E′2 and 17F′(*M*) (Table 3). As E′2(*M*) and F′(*M*) are destabilised for **16** and **17**, the number of conformations with 1-NHMe hydrogen bonds is reduced relative to the ensemble of **15**. This accounts for the observed weakening of 1-NHMe hydrogen bonds [conclusion (4) above].

Conclusions

It was shown that ferrocene-1,1′-dicarboxylic acid conjugates of types II and III form an ensemble of conformations in weakly coordinating solvents without a preference for one specific conformer. However, an increase in the steric demand of the L-amino acid side chain reduces the number of conformations [especially with respect to (*M*)-helical ferrocenes] in solution, which provides an explanation for the observed positive Cotton effect at the ferrocene absorption in the CD spectra. Furthermore, large amino acid side chains favour conformations with 1′-NH···O hydrogen bonds (conformations E/E′ and F/F′) as shown by NMR spectroscopic techniques (v.r. method) and DFT calculations.

A single hydrogen bond spanning the 1- and 1′-substituents already provides an explanation for the preference of (*P*)-helical ferrocenes in asymmetrical type II and III conjugates with one L-amino acid attached. This effect is even more pronounced in symmetrically substituted type I conjugates with two L-amino acids and two hydrogen bonds between the ferrocene substituents. For Fn(CO–Ala–OMe)$_2$, the energy difference between (*P*)- and (*M*)-"Herrick" conformers was calculated as 17.3 kJ mol^{-1} by DFT methods.[22] However, in these systems, an increase in the number of L-amino acids has no further stabilising effect.

On the basis of the results obtained in this study, it is expected that an increase in the size of the amino acid side chains adjacent to the ferrocene carbonyl might be a means to further stabilise chiral secondary structures, for example, turn motifs.

Experimental Section

General: The syntheses were carried out under an atmosphere of argon. CH_2Cl_2 that was used for syntheses and FTIR spectroscopy was dried (P_2O_5), distilled from CaH_2 and stored over molecular sieves (4 Å). EDC, HOBt (Aldrich) and amino acid esters and amides (Merck) were used as received. NMR spectroscopic data for compounds **1**–**5** were taken from refs.[25,26]. Products were purified by preparative thin layer chromatography on silica gel (Merck, Kieselgel 60 HF_{254}) by using CH_2Cl_2/EtOAc or CH_2Cl_2/MeOH. Melting points were determined with a Buechi apparatus. IR spectra were recorded as CH_2Cl_2 solutions with a Bomem MB 100 mid FTIR spectrophotometer. ^{1}H- and ^{13}C{^{1}H}-NMR spectra were recorded with a Varian EM 360 or Varian Gemini 300 spectrometer in $CDCl_3$ and [D_6]DMSO solutions with Me_4Si as the internal standard or with a Varian Unity Plus 400 spectrometer. ESI mass spectra were recorded with a Finnigan TSQ 700 spectrometer. High resolution FAB mass spectra were recorded with a JEOL JMS-700. CD spectra were recorded as CH_3CN solutions with CD spectrophotometer Jasco-810. 1′-(Methoxycarbonyl)ferrocene-1-carboxylic acid (**6**) was prepared according to a literature procedure.[30]

Computational Method: Density functional calculations were carried out with the Gaussian03/DFT[31] series of programs. The B3LYP formulation of density functional theory was used by employing the LanL2DZ basis set.[31] All points were characterised as minima (N_{imag} = 0) by frequency analysis.

Methyl 1′-(methylcarbamoyl)ferrocene-1-carboxylate (7): EDC (1.7 g, 9.1 mmol) and HOBt (1.2 g, 9.1 mmol) were added to a suspension of 1′-(methoxycarbonyl)ferrocene-1-carboxylic acid (**6**; 2 g, 7 mmol) in dry dichloromethane (20 mL), and the solution was stirred for 1 h at room temp. $MeNH_2$·HCl (682.5 mg, 10.5 mmol) was suspended in dichloromethane (5 mL) at 0 °C and dissolved by the addition of dry NEt_3 until ca. pH 8. This solution was added to the solution of activated **6**. After stirring for 1 h at room temp., the reaction mixture was washed with saturated aqueous $NaHCO_3$ and water. The organic layer was dried with Na_2SO_4 and evaporated in vacuo. TLC purification of the crude product with CH_2Cl_2/EtOAc (10:1) gave 900 mg (45%) of orange crystals. M.p. 135–

137 °C. ^{1}H NMR (300 MHz, $CDCl_3$): δ = 6.16 (br. s, 1 H, NH), 4.77 (pt, 2 H, $H^{2,5}$), 4.59 (pt, 2 H, $H^{2',5'}$), 4.46 (pt, 2 H, $H^{3,4}$), 4.37 (pt, 2 H, $H^{3',4'}$), 3.85 (s, 3 H, $COOCH_3$), 2.98 (d, $^3J_{HH}$ = 4.9 Hz, 3 H, $NHCH_3$) ppm. ^{1}H NMR (300 MHz, [D_6]-DMSO): δ = 7.75 (br. q, 1 H, NH), 4.80 (s, 2 H, $H^{2,5}$), 4.71 (s, 2 H, $H^{2',5'}$), 4.44 (s, 2 H, $H^{3,4}$), 4.36 (s, 2 H, $H^{3',4'}$), 3.71 (s, 3 H, $COOCH_3$), 2.32 (d, $^3J_{HH}$ = 4.5 Hz, 3 H, $NHCH_3$) ppm. ^{13}C NMR, APT (75 MHz, $CDCl_3$): δ = 172.0 (s, $COOCH_3$), 169.72 (s, C=O), 78.66 (s, $C^{1'}$), 71.99 (s, C^1), 72.64 (s, $C^{2,5}$), 71.84 (s, $C^{2',5'}$), 71.31 (s, $C^{3,4}$), 70.06 (s, $C^{3',4'}$), 51.96 (s, OCH_3), 26.55 (s, $NHCH_3$) ppm. IR (CH_2Cl_2): $\tilde{\nu}$ = 3462 (s, NH, free), 3373 (vw, NH, assoc.), 1712 (s, CO_{ester}), 1659 (s, amide I) 1606 (m), 1530 (s, amide II) cm^{-1}.

1′-(Methylcarbamoyl)ferrocene-1-carboxylic acid (8): A solution of NaOH (140 mg, 3.5 mmol) in water (5 mL) was added to a solution of amide ester **7** (900 mg, 3 mmol) in methanol (20 mL). After heating to 80 °C for 50 min, the reaction mixture was extracted with CH_2Cl_2. The alkaline aqueous layer was treated with conc. HCl (pH = 1–2), extracted with EtOAc and washed with water. The organic layer was dried with Na_2SO_4 and evaporated in vacuo to afford 840 mg (97%) of orange crystals. M.p. 146–149 °C. IR (KBr): $\tilde{\nu}$ = 3334 (s, NH), 3089 (s, OH), 1676 (s, CO_{acid}), 1637 (s, amide I), 1550 (s, amide II) cm^{-1}.

MeNHCO–Fn–CO–AA–OMe (9–11): Compound **8** (200 mg, 0.7 mmol) was activated by using EDC/HOBt (as described for the preparation of **7**). The solution was cooled to 0 °C and AA–OMe (obtained from AA–OMe·HCl by treatment with NEt_3 in CH_2Cl_2, pH ca. 8) was added. The reaction mixture was stirred for 1 h at room temp., washed thrice with a saturated aqueous solution of $NaHCO_3$, 10% aqueous solution of citric acid, and H_2O. After drying over Na_2SO_4 and evaporating in vacuo, the crude products were TLC-purified with EtOAc as eluent. **9** (AA = Gly): Yield: 110 mg (42%), orange crystals. M.p. 149–152 °C. ^{13}C NMR, APT (75 MHz, $CDCl_3$): δ = 170.49 (s, $CONHCH_3$), 170.48 (s, $COOCH_3$), 170.44 (s, C=O), 78.07 (s, $C^{1'}$), 76.62 (s, C^1), 70.69 (s, $C^{2,5}$), 70.59 (s, $C^{2',5'}$), 70.40 (s, $C^{3,4}$), 70.29 (s, $C^{3',4'}$), 51.85 (s, OCH_3), 40.85 (s, CH_{2Gly}), 26.07 (s, $NHCH_3$) ppm. IR (CH_2Cl_2): $\tilde{\nu}$ = 3446 (m, NH, free), 3259 (w, NH, assoc.), 1742 (s, CO_{ester}) 1650 (s, amide I), 1609 (m), 1535 (s, amide II) cm^{-1}. IR (KBr): $\tilde{\nu}$ = 3401 (s, NH, free), 3273 (s, NH, assoc.), 1737 (s, CO_{ester}), 1634 (s, amide I), 1540 (s, amide II) cm^{-1}. MS (ESI+, CH_3CN): *m*/*z* (%) = 359.3 (100) [M + H]$^+$, 381.3 (7) [M + Na]$^+$, 397.2 (5) [M + K]$^+$, 717.3 (14) [2M + H]$^+$, 739.3 (4) [2M + Na]$^+$, 755.3 (2) [2M + K]$^+$. HRMS (FAB): calcd. for $C_{16}H_{18}FeN_2O_4$ 358.0616; found 358.0619. **10** (AA = L-Ala): Yield: 157 mg (61%), orange resin. ^{13}C NMR, APT (75 MHz, $CDCl_3$): δ = 174.25 (s, $COOCH_3$), 170.82 (s, $CONHCH_3$), 170.39 (s, C=O), 78.54 (s, $C^{1'}$), 76.75 (s, C^1), 71.37 (s, C^2), 71.32 (s, C^5), 71.28 (s, $C^{2'}$), 71.26 (s, $C^{5'}$), 70.89 (s, C^3), 70.83 (s, C^4), 70.77 (s, $C^{3'}$), 70.09 (s, $C^{4'}$), 52.57 (s, OCH_3), 48.39 (s, CH_{Ala}), 26.58 (s, $NHCH_3$), 17.71 (s, CH_{3Ala}) ppm. IR (CH_2Cl_2): $\tilde{\nu}$ = 3451 (m, NH, free), 3271 (w, NH, assoc.), 1740 (s, CO_{ester}), 1650 (s, amide I), 1534 (s, amide II) cm^{-1}. MS (ESI+, CH_3CN): *m*/*z* (%) = 373.3 (100) [M + H]$^+$, 395.3 (18) [M + Na]$^+$, 411.3 (21) [M + K]$^+$, 745.3 (8) [2M + H]$^+$, 767.3 (14) [2M + Na]$^+$, 783.2 (6) [2M + K]$^+$. HRMS (FAB): calcd. for $C_{17}H_{20}FeN_2O_4$ 372.0773; found 372.0766. **10a** (AA = D-Ala): Yield: 54%, orange resin. NMR and IR spectra of **10a** were similar to those of **10**. **11** (AA = L-Val): Yield: 130 mg (46%), orange resin. ^{13}C NMR, APT (75 MHz, $CDCl_3$): δ = 173.28 (s, $COOCH_3$), 170.72 (s, $CONHCH_3$), 170.57 (s, C=O), 78.69 (s, $C^{1'}$), 76.81 (s, C^1), 71.51 (s, C^2), 71.38 (s, $C^{2',5}$), 71.12 (s, $C^{3,5'}$), 70.83 (s, C^4), 70.25 (s, $C^{3'}$), 70.07 (s, $C^{4'}$), 57.53 (s, $CH\alpha_{Val}$), 52.34 (s, OCH_3), 30.73 (s, $CH\beta_{Val}$), 26.55 (s, $NHCH_3$), 19.20 (s, CH_{3Val}), 18.19 (s, CH_{3Val}) ppm. IR (CH_2Cl_2): $\tilde{\nu}$ = 3453, 3418 (m, NH, free), 3293 (w, NH, assoc.), 1736 (s, CO_{ester}), 1665 (s, amide I), 1520 (s, amide II) cm^{-1}. MS (ESI+, CH_3CN): *m*/*z* (%) = 401.3 (100) [M + H]$^+$, 423.3 (28) [M + Na]$^+$, 439.3 (18) [M + K]$^+$, 801.4 (5) [2M + H]$^+$, 823.3 (17) [2M + Na]$^+$, 839.2 (7) [2M + K]$^+$. HRMS (FAB): calcd. for $C_{19}H_{24}FeN_2O_4$ 400.1085; found 400.1073.

MeNHCO–Fn–CO–AA–OH (12–14): MeNHCO–Fn–CO–AA–OMe (**9**–**11**, 0.3 mmol) was dissolved in a mixture of dioxane (10 mL) and water (10 mL). After cooling to 10 °C and the ad-

Table 4. ^{1}H NMR chemical shifts for **9**–**11** and **15**–**17** in $CDCl_3$.

	9	**10**	**11**	**15**	**16**	**17**
1-N*H*	7.39 (1 H, br. t)	7.03 (d, 1 H, *J* = 7.0 Hz)	6.63 (d, 1 H, *J* = 8.4 Hz)	7.15 (1 H, br. t)	6.77 (d, 1 H, *J* = 6.8 Hz)	6.52 (1 H, br. d, *J* = 7.9 Hz)
1′-N*H*	6.72 (1 H, br. q)	6.88 (1 H, br. q)	7.03 (1 H, br. q)	6.89 (1 H, br. q)	7.08 (1 H, br. q)	7.20 (1 H, br. q)
1-N*H*CH_3	–	–	–	6.86 (1 H, br. q)	6.71 (1 H, br. q)	6.55 (1 H, br. q)
C*Hα*	4.13 (d, 2 H, *J* = 5.8 Hz)	4.62 (m, 1 H)	4.61 (m, 1 H)	4.03 (d, 2 H, *J* = 5.8 Hz)	4.55 (m, 1 H)	4.32 (m, 1 H)
Cp-*H*	4.69 (2 H, pt) 4.53 (2 H, pt) 4.38 (4 H, pt)	4.73 (1 H, pt) 4.63 (1 H, pt) 4.58 (1 H, pt) 4.44 (1 H, pt) 4.39 (m, 2 H) 4.36 (1 H, pt) 4.33 (1 H, pt)	4.62 (1 H, pt) 4.60 (m, 2 H) 4.43 (1 H, pt) 4.41 (1 H, pt) 4.38 (1 H, pt) 4.36 (1 H, pt) 4.32 (1 H, pt)	4.64 (2 H, pt) 4.59 (2 H, pt) 4.40 (2 H, pt) 4.37 (2 H, pt)	4.68 (1 H, pt) 4.65 (1 H, pt) 4.57 (1 H, pt) 4.44 (1 H, pt) 4.42 (1 H, pt) 4.39 (1 H, pt) 4.36 (1 H, pt) 4.32 (1 H, pt)	4.69 (m, 2 H) 4.51 (1 H, pt) 4.48 (1 H, pt) 4.41 (1 H, pt) 4.36 (1 H, pt) 4.35 (1 H, pt) 4.31 (1 H, pt)
1′-NHC*H*$_3$	2.91 (d, 3 H, *J* = 4.8 Hz)	2.91 (d, 3 H, *J* = 4.8 Hz)	2.95 (d, 3 H, *J* = 4.7 Hz)	2.90 (d, 3 H, *J* = 4.7 Hz)	2.95 (d, 3 H, *J* = 4.7 Hz)	2.94 (d, 3 H, *J* = 4.7 Hz)
OC*H*$_3$/ 1-NHC*H*$_3$	3.78 (s, 3 H)	3.78 (s, 3 H)	3.82 (s, 3 H)	2.86 (d, 3 H, *J* = 4.7 Hz)	2.87 (d, 3 H, *J* = 4.7 Hz)	2.87 (d, 3 H, *J* = 4.7 Hz)
R	–	1.51 (d, 3 H, *J* = 7.3 Hz)	2.11 (m, 1 H) 1.04 (d, 3 H, *J* = 6.7 Hz) 1.02 (d, 3 H, *J* = 6.7 Hz)	–	1.47 (d, 3 H, *J* = 6.8 Hz)	2.16 (m, 1 H) 1.01 (d, 3 H, *J* = 6.7 Hz) 1.00 (d, 3 H, *J* = 6.7 Hz)

Table 5. ^{1}H NMR chemical shifts for **9**–**11** and **15**–**17** in [D$_6$]DMSO.

	9	**10**	**11**	**15**	**16**	**17**
1-N*H*	8.40 (1 H, br. t, *J* = 5.2 Hz)	8.24 (d, 1 H, *J* = 6.9 Hz)	7.88 (d, 1 H, *J* = 7.9 Hz)	8.17 (t, 1 H, *J* = 5.9 Hz)	7.88 (1 H, br. d, *J* = 7.4 Hz)	7.65 (1 H, br. d, *J* = 8.6 Hz)
1′-N*H*	7.73 (1 H, br. q)	7.75 (1 H, br. q)	7.66 (1 H, br. q)	7.98 (1 H, br. q)	7.97 (1 H, br. q)	7.88 (1 H, br. q)
1-N*H*CH$_3$	–	–	–	7.85 (1 H, br. q)	7.91 (1 H, br. q)	8.01 (1 H, br. q)
C*Ha*	3.92 (d, 2 H, *J* = 5.7 Hz)	4.35 (m, 1 H)	4.26 (1 H, pt, *J* = 7.6 Hz)	3.74 (d, 2 H, *J* = 5.9 Hz)	4.32 (m, 1 H)	4.11 (pt, 1 H, *J* = 8.0 Hz)
Cp-*H*	4.76 (s, 2 H) 4.73 (s, 2 H) 4.38 (s, 2 H) 4.31 (s, 2 H)	4.78 (s, 1 H) 4.76 (s, 1 H) 4.71 (s, 2 H) 4.38–4.31 (m, 4 H)	4.77 (m, 3 H) 4.71 (s, 1 H) 4.34 (m, 2 H) 4.30 (m, 2 H)	4.73 (s, 2 H) 4.70 (s, 2 H) 4.38 (s, 2 H) 4.34 (s, 2 H)	4.78 (s, 1 H) 4.72 (m, 3 H) 4.36 (s, 2 H) 4.32 (s, 2 H)	4.81 (s, 1 H) 4.79 (s, 1 H) 4.70 (s, 1 H) 4.68 (s, 1 H) 4.33 (s, 1 H) 4.31 (s, 1 H) 4.28 (s, 2 H)
1′-NHC*H*$_3$	2.69 (d, 3 H, *J* = 4.2 Hz)	2.70 (d, 3 H, *J* = 4.5 Hz)	2.72 (d, 3 H, *J* = 4.6 Hz)	2.69 (d, 3 H, *J* = 4.5 Hz)	2.71 (d, 3 H, *J* = 4.5 Hz)	2.70 (d, 3 H, *J* = 4.1 Hz)
OC*H*$_3$/ 1-NHC*H*$_3$	3.67 (s, 3 H)	3.66 (s, 3 H)	3.67 (s, 3 H)	2.64 (d, 3 H, *J* = 4.5 Hz)	2.63 (d, 3 H,*J* = 4.5 Hz)	2.61 (d, 3 H, *J* = 4.2 Hz)
R	–	1.39 (d, 3 H, *J* = 7.3 Hz)	2.18 (m, 1 H) 1.01 (d, 3 H, *J* = 6.8 Hz) 0.96 (d, 3 H, *J* = 6.8 Hz)	–	1.30 (d, 3 H, *J* = 7.2 Hz)	2.07 (m, 1 H) 0.94 (d, 3 H, *J* = 6.6 Hz) 0.89 (d, 3 H, *J* = 6.7 Hz)

dition of NaOH (23 mg, 0.6 mmol), the reaction mixture was stirred at room temp. for 10 min. The solution was treated with conc. HCl to pH = 2–3, extracted with EtOAc, washed with saturated aqueous $NaHCO_3$ and water. The organic layer was dried with Na_2SO_4 and evaporated in vacuo. Compounds **12**–**14** were used without purification for further transformation. **12** (AA = Gly): Yield: 100 mg (94%), orange crystals. M.p. 115–117 °C. IR (KBr): $\tilde{\nu}$ = 3458 (m, NH, free), 3092 (s, OH), 1630 (s, amide I), 1534 (s, amide II) cm^{-1}. **13** (AA = L-Ala): Yield: 94 mg (81%), orange resin. IR (CH_2Cl_2): $\tilde{\nu}$ = 3450 (m, NH, free), 3100 (s, OH), 1655 (s, amide I), 1534 (s, amide II) cm^{-1}. **14** (AA = L-Val): Yield: 96 mg (94%), orange resin. IR (CH_2Cl_2): $\tilde{\nu}$ = 3453 (m, NH, free), 3110 (s, OH), 1650 (s, amide I), 1534 (s, amide II) cm^{-1}.

MeNHCO–Fn–CO–AA–NHMe (15–17). Procedure A: MeNHCO–Fn–CO–AA–OH (**12**–**14**; 0.25 mmol) was activated (as described for **7**) and reacted with $MeNH_2$·HCl (cf. preparation of **9**–**11**). The crude products were purified by TLC using EtOAc as the eluent to give orange resins **15** (24%), **16** (56%) and **17** (20%), respectively. **Procedure B:** Acid amide **8** (150 mg, 0.526 mmol) was activated by using EDC/HOBt as described for **7** and reacted with AA–NHMe (obtained from AA–NHMe·HCl similarly as in preparation of **9**–**11**). The products were purified by TLC using EtOAc as the eluent to give orange resins **15** (45%), **16** (45%), **17** (34%). The compounds prepared by these alternative procedures display identical NMR and IR spectra. **15** (AA = Gly): orange resin. ^{13}C NMR, APT (75 MHz, $CDCl_3$): δ = 170.31 (s, $CONHCH_3$), 170.22 (s, $CONHCH_3$), 169.72 (s, C=O), 77.75 (s, C$^{1'}$), 76.25 (s, C^1), 70.93 (s, C^{2,5}), 70.75 (s, C$^{2',5'}$), 70.12 (s, C^{3,4}), 69.92 (s, C$^{3',4'}$), 43.01 (s, CH_{2Gly}), 26.08 (s, $NHCH_3$), 25.85 (s, $NHCH_3$) ppm. IR (CH_2Cl_2): $\tilde{\nu}$ = 3449 (m, NH, free), 3341 (w, NH, assoc.), 1655 (s, amide I), 1607 (s), 1534 (s, amide II) cm^{-1}. MS (ESI+, CH_3CN): *m*/*z* (%) = 358.4 (100) [M + H]$^+$, 380.4 (5) [M + Na]$^+$, 715.3 (4) [2M + H]$^+$, 737.5 (3) [2M + Na]$^+$. HRMS (EI): calcd. for $C_{16}H_{19}FeN_3O_3$ 357.0776; found 357.0754. **16** (AA = L-Ala): orange resin. ^{13}C NMR, APT (75 MHz, $CDCl_3$): δ = 173.80 (s, $CONHCH_3$), 170.69 (s, $CONHCH_3$), 170.32 (s, C=O), 78.16 (s, C$^{1'}$), 76.40 (s, C^1), 71.59 (s, C^2), 71.38 (s, C^5), 71.34 (s, C$^{2'}$) 71.01 (s, C$^{5'}$), 70.65 (s, C^3), 70.62 (s, C^4), 70.58 (s, C$^{3'}$), 70.19 (s, C$^{4'}$), 49.47 (s, CH_{Ala}), 26.62 (s, $NHCH_3$), 26.48 (s, $NHCH_3$), 18.18 (s, CH_{3Ala}) ppm. IR (CH_2Cl_2): $\tilde{\nu}$ = 3449 (m, NH, free), 3363, 3327 (m, NH, assoc.), 1653 (s, amide I), 1536 (s, amide II) cm^{-1}. MS (ESI+, CH_3CN): *m*/*z* (%) = 372.3 (100) [M + H]$^+$, 394.3 (2) [M + Na]$^+$, 410.4 (4) [M + K]$^+$, 743.3 (21) [2M + H]$^+$, 765.2 (5) [2M + Na]$^+$, 781.2 (3) [2M + K]$^+$. HRMS (FAB): calcd for $C_{17}H_{21}FeN_3O_3$ 371.0932; found 371.0965. **17** (AA = L-Val): orange resin. ^{13}C NMR, APT (75 MHz, $CDCl_3$): δ = 172.68 (s, $CONHCH_3$), 170.65 (s, $CONHCH_3$), 170.60 (s, C=O), 78.13 (s, C$^{1'}$), 76.8 (s, C^1), 71.67 (s, C^2) 71.39 (s, C^5), 71.31 (s, C$^{2',5'}$), 71.15 (s, C^3) 70.91 (s, C^4), 69.87 (s, C$^{3'}$) 69.74 (s, C$^{4'}$), 59.34 (s, CH_{Val}), 30.74 (s, CH_{Val}), 26.64 (s, $NHCH_3$), 26.40 (s, $NHCH_3$), 19.51 (s, CH_{3Val}), 18.53 (s, CH_{3Val}) (Tables 4, 5 and 6) ppm. IR (CH_2Cl_2): $\tilde{\nu}$ = 3451 (m, NH, free), 3342, 3326 (m, NH, assoc.), 1657 (s, amide I), 1605 (m), 1532 (s, amide II) cm^{-1}. MS (ESI+, CH_3CN): *m*/*z* (%) = 400.4 (100) [M + H]$^+$, 422.4 (24) [M + Na]$^+$, 438.3 (4) [M + K]$^+$, 799.4 (9) [2M + H]$^+$, 821.3 (4) [2M + Na]$^+$, 837.3 (2) [2M + K]$^+$. HRMS (FAB): calcd for $C_{19}H_{25}FeN_3O_3$ 399.1245; found 399.1227.

Table 6. UV/Vis and CD data for **10**, **11**, **16** and **17** in CH_3CN.

	λ_{max} / nm	λ_{max} / nm (M_θ / °M^{-1}cm^{-1})
10	452	299 (340), 349 (–220), 411 (–120), 471 (360)
10a	442	300 (–260), 350 (170), 413 (90), 475 (–250)
11	439	301 (360), 347 (–330), 411 (–190), 470 (430)
16	452	305 (810), 352 (–340), 419 (–190), 483 (410)
17	444	305 (860), 352 (–480), 415 (–270), 479 (530)

Supporting Information (see footnote on the first page of this article): DFT calculated cartesian coordinates for all conformers of **9**, **10**, **11**, **15**, **16** and **17**.

Acknowledgments

The authors are grateful to Ph. D. Dinko Žiher, GlaxoSmithKline Research Centre Zagreb, Ltd., for the CD measurements. We thank

the Ministry for Science, Education and Sport of Croatia for support through a grant and the German Science Foundation for a Heisenberg fellowship (to K. H.).

[1] S. Chowdhury, D. A. R. Sanders, G. Schatte, H.-B. Kraatz, *Angew. Chem.* **2006**, *118*, 765–768; *Angew. Chem. Int. Ed.* **2006**, *45*, 751–754.
[2] T. Moriuchi, T. Nagai, T. Hirao, *Org. Lett.* **2005**, *7*, 5265–5268.
[3] S. I. Kirin, D. Wissenbach, N. Metzler-Nolte, *New J. Chem.* **2005**, *29*, 1168–1173.
[4] S. Chowdhury, G. Schatte, H.-B. Kraatz, *Dalton Trans.* **2004**, 1726–1730.
[5] F. E. Appoh, T. C. Sutherland, H.-B. Kraatz, *J. Organomet. Chem.* **2004**, *689*, 4669–4677.
[6] T. Moriuchi, K. Yoshida, T. Hirao, *Org. Lett.* **2003**, *5*, 4285–4288.
[7] T. Moriuchi, A. Nomoto, K. Yoshida, T. Hirao, *Organometallics* **2001**, *20*, 1008–1013.
[8] T. Moriuchi, A. Nomoto, K. Yoshida, A. Ogawa, T. Hirao, *J. Am. Chem. Soc.* **2001**, *123*, 68–75.
[9] T. Moriuchi, A. Nomoto, K. Yoshida, T. Hirao, *J. Organomet. Chem.* **1999**, *589*, 50–58.
[10] A. Nomoto, T. Moriuchi, S. Yamazaki, A. Ogawa, T. Hirao, *Chem. Commun.* **1998**, 1963–1964.
[11] R. S. Herrick, R. M. Jarret, T. P. Curran, D. R. Dragoli, M. B. Flaherty, S. E. Lindyberg, R. A. Slate, L. C. Thornton, *Tetrahedron Lett.* **1996**, *37*, 5289–5292.
[12] D. R. van Staveren, T. Weyhermüller, N. Metzler-Nolte, *Dalton Trans.* **2003**, 210–220.
[13] X. de Hatten, T. Weyhermüller, N. Metzler-Nolte, *J. Organomet. Chem.* **2004**, *689*, 4856–4867.
[14] Y. Xu, P. Saweczko, H.-B. Kraatz, *J. Organomet. Chem.* **2004**, *689*, 4669–4677.
[15] Y. Xu, P. Saweczko, H. B. Kraatz, *J. Organomet. Chem.* **2001**, *637–639*, 335–342.
[16] M. Oberhoff, L. Duda, J. Karl, R. Mohr, G. Erker, R. Fröhlich, M. Grehl, *Organometallics* **1996**, *15*, 4005–4011.
[17] S. I. Kirin, H.-B. Kraatz, N. Metzler-Nolte, *Chem. Soc. Rev.* **2006**, *35*, 348–354.
[18] A. Kuik, R. Skoda-Földes, A. C. Benyei, G. Rangits, L. Kollar, *J. Organomet. Chem.* **2006**, *691*, 3037–3042.
[19] K. Heinze, M. Beckmann, *Eur. J. Inorg. Chem.* **2005**, 3450–3457.
[20] E. Vass, M. Hollósi, F. Besson, R. Buchet, *Chem. Rev.* **2003**, *103*, 1917–1954.
[21] K. Heinze, M. Schlenker, *Eur. J. Inorg. Chem.* **2004**, 2974–2988.
[22] S. I. Kirin, U. Schatzschneider, X. de Hatten, T. Weyhermüller, N. Metzler-Nolte, *J. Organomet. Chem.* **2006**, *691*, 3451–3457.
[23] K. Heinze, M. Beckmann, *J. Organomet. Chem.* **2006**, *691*, 5588–5596.
[24] K. Heinze, U. Wild, M. Beckmann, *Eur. J. Inorg. Chem.* **2007**, 617–623.
[25] Y. Jin, K. Tonan, S. Ikawa, *Spectrochim. Acta Part A* **2002**, *58*, 2795–2802.
[26] L. Barišić, M. Čakić, K. A. Mahmoud, Y. Liu, H.-B. Kraatz, H. Pritzkow, S. I. Kirin, N. Metzler-Nolte, V. Rapić, *Chem. Eur. J.* **2006**, *12*, 4965–4980.
[27] L. Barišić, V. Rapić, V. Kovač, *Croat. Chem. Acta* **2002**, *75*, 199–210.
[28] a) L. Barišić, M. Dropučić, V. Rapić, H. Pritzkow, S. I. Kirin, N. Metzler-Nolte, *Chem. Commun.* **2004**, 2004–2005; b) S. Chowdhury, G. Schatte, H.-B. Kraatz, *Angew. Chem.* **2006**, *118*, 7036–7038; *Angew. Chem. Int. Ed.* **2006**, *45*, 6882–6884.
[29] L. Barišić, V. Rapić, N. Metzler-Nolte, *Eur. J. Inorg. Chem.* **2006**, 4019–4021.
[30] A. Sonda, I. Martini, *J. Organomet. Chem.* **1971**, *26*, 133–140.
[31] M. J. Frisch, G. W. Trucks, H. B. Schlegel, G. E. Scuseria, M. A. Robb, J. R. Cheeseman, J. A. Montgomery Jr, T. Vreven, K. N. Kudin, J. C. Burant, J. M. Millam, S. S. Iyengar, J. Tomasi, V. Barone, B. Mennucci, M. Cossi, G. Scalmani, N. Rega, G. A. Petersson, H. Nakatsuji, M. Hada, M. Ehara, K. Toyota, R. Fukuda, J. Hasegawa, M. Ishida, T. Nakajima, Y. Honda, O. Kitao, H. Nakai, M. Klene, X. Li, J. E. Knox, H. P. Hratchian, J. B. Cross, C. Adamo, J. Jaramillo, R. Gomperts, R. E. Stratmann, O. Yazyev, A. J. Austin, R. Cammi, C. Pomelli, J. W. Ochterski, P. Y. Ayala, K. Morokuma, G. A. Voth, P. Salvador, J. J. Dannenberg, V. G. Zakrzewski, S. Dapprich, A. D. Daniels, M. C. Strain, O. Farkas, D. K. Malick, A. D. Rabuck, K. Raghavachari, J. B. Foresman, J. V. Ortiz, Q. Cui, A. G. Baboul, S. Clifford, J. Cioslowski, B. B. Stefanov, G. Liu, A. Liashenko, P. Piskorz, I. Komaromi, R. L. Martin, D. J. Fox, T. Keith, M. A. Al-Laham, C. Y. Peng, A. Nanayakkara, M. Challacombe, P. M. W. Gill, B. Johnson, W. Chen, M. W. Wong, C. Gonzalez, J. A. Pople, *Gaussian 03*, Revision B.03, Gaussian, Inc., Pittsburgh PA, **2003**.

Received: December 22, 2006
Published Online: March 23, 2007

